PHILOSOPHICAL TRANSACTIONS A

rsta.royalsocietypublishing.org

Research

Article submitted to journal

Subject Areas:
Civil Engineering, Renewable energy, Sediment transport

Keywords:
Tidal power, Resource assessment, Sandbanks, Sediment transport, Channel Islands

Author for correspondence:
Luke Blunden
e-mail: lsb1@soton.ac.uk

Tidal current power effects on nearby sandbanks: a case study in the Race of Alderney

L. S. Blunden[1], S. G. Haynes[1] and A. S. Bahaj[1]

[1]Sustainable Energy Research Group, Energy and Climate Change Division, Faculty of Engineering and Physical Sciences, University of Southampton, UK, SO16 7QF

A validated numerical model of tidal flows and sediment transport around the Alderney South Banks was used to investigate the potential effects of large (300 MW) tidal turbine arrays at different locations in Alderney territorial waters. Two methods were used, firstly looking at hydrodynamic changes only and secondly modelling sediment transport over a non-erodible bed. The baseline hydrodynamic model was validated relative to ADCP velocity data collected in the immediate vicinity of the sandbank. Real-world sand transport rates were inferred from sand-wave migrations and agree favourably with sediment transport residuals calculated from model outputs. Outputs from the sediment model reproduced realistic morphological behaviours over the bank. Seventeen different locations were considered; most did not result in significant hydrodynamic changes over the South Banks, however three array locations were singled out as requiring extra caution if development were to occur. The results provide a case for optimizing the array locations for twin objectives of maximizing array power and minimizing impacts on the sandbanks.

1. Introduction

Fast tidal currents of interest for power generation often occur close to islands or headlands, where flow separation can occur and cause large areas of recirculation, extending over many kilometres. This is the case for a number of sites identified as having high potential for development,

THE ROYAL SOCIETY PUBLISHING

notably the Pentland Firth to the south of the island of Stroma [1–3]; at Portland [4] (a headland on the south coast of the UK) and Alderney [5] (an island in the Normandy-Brittany Gulf). In all these locations, large submerged sandbanks exist within a few hundred meters of flows that exceed 3 m/s at spring tides; flows that could easily remove the sand, if diverted onto the banks.

Numerical modelling of these sandbanks in their natural state is a challenge due to the large range of temporal and spatial scales involved along with many uncertain parameters; extending such models to include large arrays of tidal turbines is even more challenging due to the uncertainties in tidal array parameterization. Nevertheless, it is important to be able to assess the likely impacts on sandbanks of potential tidal power developments nearby. Sandbanks are of ecological significance, their precise location is important for safe navigation and they may also protect against shoreline erosion [6].

Sediment transport in the context of energy extraction by arrays of tidal turbines was considered first by [7], who investigated changes in the Bristol Channel using a 1-D model. It was shown that energy extracted from regions of strong tidal asymmetry led to a 20% increase in the magnitude of bed-level changes (when averaged over the length of the model) compared to the tidal symmetry cases. The study suggested that tidal turbine arrays located in sites exhibiting a strong tidal asymmetry will have a much larger impact upon the long-term sediment dynamics of a region than those located in areas of tidal symmetry. A 3-D model was used by [5] for a case study of a 300 MW array close to Alderney which demonstrated the potential for tidal arrays to causeeither accretion or erosion of the Alderney South Banks, depending on siting of the arrayy. In a more detailed study, [8] investigated the natural variability of sediment transport in the vicinity of the Skerries (Angelsey, UK) compared with that due to tidal energy extraction, using field survey data, a coupled sediment transport module and a separate wave model. It was found that for tidal arrays of up to 50 MW, changes to sediment transport were less than the natural variability.

The Race of Alderney (or Raz Blanchard) has been the subject of interest for tidal power generation for many years [9,10] with estimates of average annual power generation varying from 40 MW to 4 GW [11,12]. It has also been the subject of two sediment transport modelling studies in the context of tidal power. The first, [5] did not have access to the high resolution bathymetry or flow data used in this study. The second, [13] investigated a 290 MW array in French waters on the eastern side of the Race and did not specifically consider the South Banks, focussing instead on the wider sediment transport regime of the English Channel.

(a) Sandbank development in fast tidal flows

A comprehensive review of the origin of sandbanks was given by [14], in which a general typology was proposed that is briefly summarized in Table 1. The main type of sandbank in the context of tidal power development—Type 3A sandbanks —are formed at headlands where sediment transported by long-shore drift (from one or both sides of the headland) is swept offshore where it accumulates to form a long, linear sandbank. Tidal flows around the headland are a key factor in the formation of Type 3 sandbanks. Strong currents are required to move sediment far offshore (along the length of the bank) and to form large eddies in the lee of the headland that play an important role in helping form and maintain the sandbank. Banner banks typically take the form of a straight line protruding from a coastal headland into deep water and are a consequence of the way in which tidal flows behave downstream from the headland.

Increases or decreases to the magnitudes of the residual sediment transport could modify the shape of the sandbank with newly created sediment convergence zones and subsequent modifications to the sandbank shape. Although modification of just the residual magnitudes could alter the sandbanks equilibrium profile it would seem that a reversal in the sediment transport residual direction at any point on the bank could have a very significant impact upon the morphology. If the sand circulation was reduced dramatically or even reversed at any point along either flank of the bank then the long-term equilibrium of the bank would be compromised.

Table 1: Summary of types of sandbank observed on continental shelves. Derived from [14]

Type			Name	Description
1			Open shelf ridges	Occur widely in open shallow shelf seas with tidal currents exceeding 0.5 m/s. May be the convergent state for all banks when separated from original context.
2	A		Estuary mouth ridges	Occur in macrotidal estuaries where the mouth is wide (>10 km), and multiple channels form parallel to currents.
	B	(i)	Ebb tidal deltas	Occur in meso- or microtidal estuaries with a narrow mouth (<10km), with a main deep channel and linear bars around it.
		(ii)	Shoreface connected ridges	As 2B(i), but inlets migrate with longshore drift, interacting with barrier beaches.
3	A		Headland associated banner banks	Occur where sediment is trapped by flows that separate from headlands or islands, where headland retreat is slow and sediment supply limited
	B		Headland associated alternating ridges	As 3A, but in the case where the headland is actively retreating, along with the sediment supply, multiple banks can occur.

A total reversal in the residual transport at a particular location would require a large change in the ambient hydrodynamics and is unlikely. Having said this, the important role of the propagating eddy shed by the headland tip is clear from the literature [15–17]. The strength, propagation direction and life-time of the eddy could be altered significantly by localised changes in the hydrodynamic regime in the region where the eddy forms. In this way, localized changes in the flow regime could have a wider impact upon sand movement around sandbanks.

2. Site characteristics

The South Banks are collectively a 7.5 km long by 1.5 km wide submarine sandbank located to the South of the island of Alderney. The Alderney South Banks are a Type 3A 'banner' sandbank as determined using the classification system proposed by [14]. The Banks extend out from the littoral zone to depths of over 40 m and exhibit maximum heights above the surrounding bedrock strata of around 25 m. As the ebb tidal flows pass to the South of Alderney, large clockwise eddies are shed by the island tip and propagate along the line of the sandbank. At the South Banks the circulation of sand represents a consistent clockwise pathway of the residual sediment transport around the bank. Figure 1 shows the main sediment transport pathways around the South Banks, inferred from the asymmetry in cross-section between the lee and stoss faces of the bedforms [18]. It can be seen that there is a clockwise pattern of sediment circulation converging on the centreline of the Banks.

A bathymetric survey of the South Banks was carried out for the Alderney Commission for Renewable Energy in November 2010. Due to weather constraints, some transects were completed 50 days later than the original survey, in February 2011 and partly overlapped the original coverage. Although the survey was not aimed at determining bedform migration rates, the 50-day delay allowed comparison of the location of sandwave crests, from which it was clear that

the South Banks possess a complex and extremely active morphology. Significant volumes of sand are circulated around the sandbank and very high sandwave migration rates of up to 70 m in a 50 day period were observed in one part of the Bank. This is significantly higher than rates of up to 20 m/year reported in the literature for the North Sea [19,20]. It is possible that sand is supplied to the Banks from an active scour zone at the tip of the island, or from the wider sea-bed to the North-East of the island. To directly measure long term rates and directions of sediment transport within and around the Banks would require multiple bathymetric surveys over a period of months or years and this data is not presently available. Nevertheless, it is clear from depth soundings on historic charts that the Banks as a whole have been maintained in a quasi-equilibrium state for many decades. While it is not clear whether there is a sediment supply to the Banks, available survey data indicate net clockwise circulation of sediment around the centreline, which acts to maintain the Banks. Therefore changes to this important process caused by changes to the wider flow regime have the potential to affect the long-term stability of the Banks.

A sedimentary survey of the South Banks in May 2011 collected eleven sediment grab samples covering the length of the bank. A particle size analysis yielded d_{50} values (median grain size) of 0.98–2.39 mm and corresponding d_{90} values of 1.90–7.00 mm (see Figure 2 for spatial variation in grain size). These values are characterised as Very coarse sand (1–2 mm) with the most South-Westerly reading corresponding to Gravel Granules (2-4mm). There is a large variation in grain size along the length of the bank with the largest values at the South-Westerly tip. These values decrease gradually along the length of the bank towards the centre and then remain fairly constant up to the North-Eastern end. The variation is likely to occur as a result of a spatial-sorting effect whereby different grain sizes sit in a different spatial equilibrium with the surrounding hydrodynamic regime. The median grain sizes and the qualitative spatial distribution closely match that reported at Shambles Bank, Portland, UK [16].

3. Methods

(a) Baseline model

A 2-D numerical model (TELEMAC-2D [21]) was used to simulate the tidal flows in the vicinity of Alderney and across the wider English Channel. The model was driven by tidal elevations at the open boundaries using nine tidal constituents (M_2, S_2, K_1, O_1, P_1, N_2, K_2, Q_1 and M_4), derived from the OTPS software at the Atlantic boundary [22] and digitized co-tidal charts in the North Sea and Irish Sea [23]. The model mesh contained 94 k nodes and 184 k elements with a 'quasi-bubble' discretization in velocity, linear in depth. The time discretization was semi-implicit, the time step was 75 s and the model runs were parallelized on 48 processors. A constant turbulence viscosity of 10^{-4} m^2 was used and the Nikuradse roughness model applied with a spatially varying parameter k_s used to tune the model. See Figure 3 for an overview of the mesh along with roughness zones and boundary conditions. See §5 for access to configuration and boundary conditions files for the model. The model was validated against tidal elevation records obtained from port tide-gauges and tidal currents derived from ADCP deployments.

Bathymetric data used to generate the model mesh was a combination of GEBCO [24](for the areas outside the English Channel), TCarta covering the English Channel (licenced from TCarta Marine LLC and originally gridded at 50 m resolution from 1:200000 charts) and local bathymetric survey datasets of the South Banks with ≈ 2 m resolution. The datasets were combined with smooth spline interpolation at the boundaries between higher and lower resolution areas in order to avoid artificial discontinuities in depth. Typical mesh edge length varied from 115 m in the vicinity of Alderney South Banks to 8 km on the mesh open boundaries. The sandwaves superimposed upon the South Banks were smoothed out of the bathymetric data using a spatial moving-average approach which preserved the total volume of sand to within 2% of the original value.

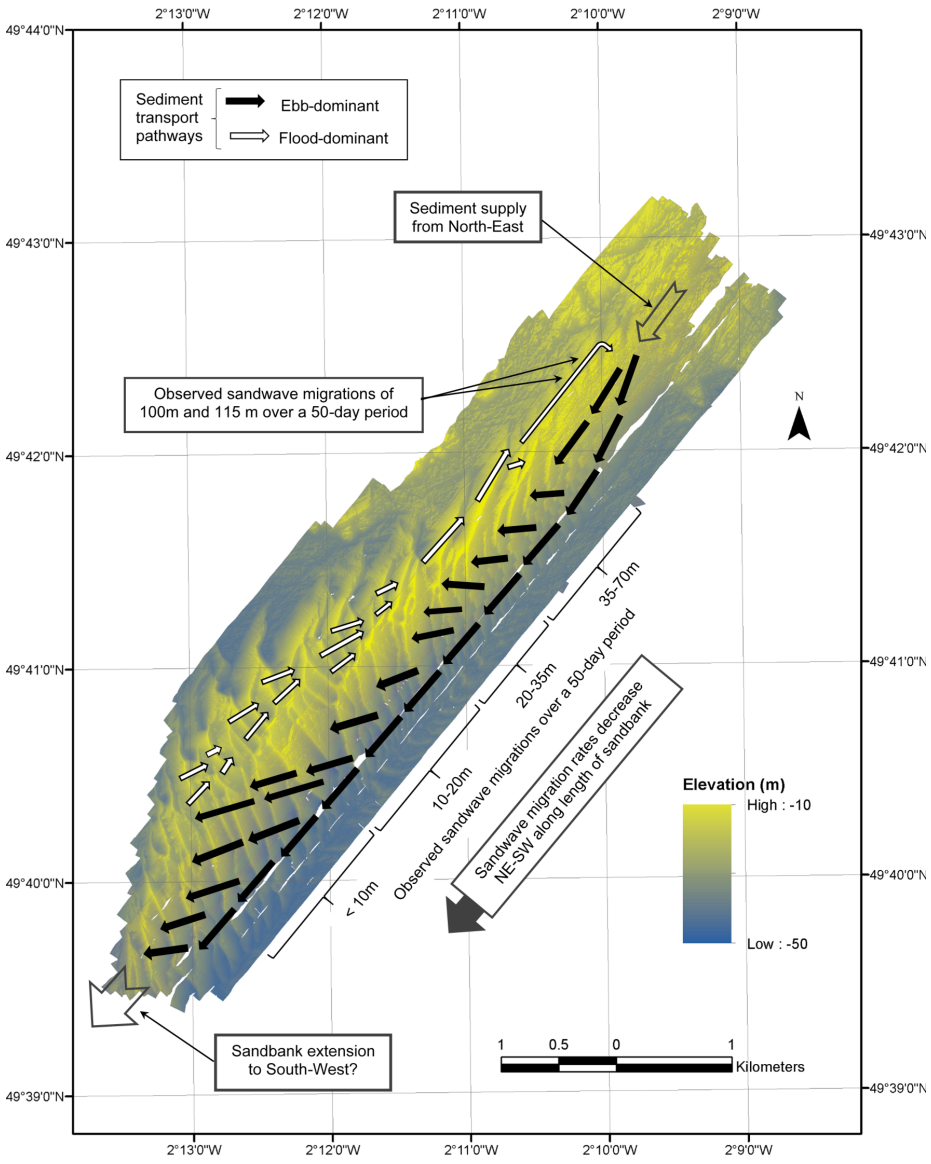

Figure 1: Observed sandwave migration rates in the context of the bathymetry of Alderney South Banks

(b) Energy extraction approach

An existing, area-averaged roughness method for parameterizing the effects of energy extraction for tidal arrays was incorporated into the model [25]. The notional array represented by the applied roughness was 150 turbines of rated capacity 2 MW and 16 m diameter, spaced at 11.3 diameters in the primary flow direction and 4.2 diameters laterally, within an overall footprint of 1.8 km (in the direction of flow) by 1.0 km (see Table 2 for summary of array parameters). Baseline and energy-extraction models were set up identically (model-run time, tidal boundary forcing, other parameters all kept the same) with the exception of the added drag force representing the

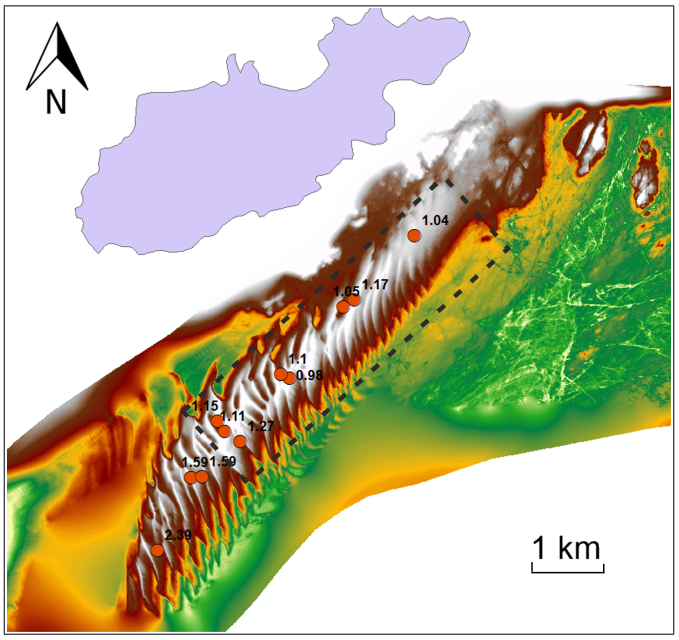

Figure 2: Median grain size d_{50} (mm) as determined from grab samples collected at 11 locations along the length of the South Banks. The dotted line indicates the area across which grain size values were averaged for use in the sediment model, for more details see §3(c).

arrays. Extraction outputs were then subtracted from the baseline velocity for the hydrodynamic model, to quantify the spatial and time-varying impact of each extraction scenario. These velocity differences were then used to assess the likely impact of each energy extraction scenario upon the South Banks' morphology.

Table 2: Tidal array parameters

Parameter	Symbol	Value	Unit
Number of turbines	N	150	—
Turbine diameter	D	16	m
Longitudinal spacing	L_x/D	11.3	—
Lateral spacing	L_y/D	4.2	—
Turbine rated flow speed	U_r	3.5	m/s
Turbine drag coefficient	c_d	0.9	—
2D drag coefficient	c_d'	0.57	—

(c) Static bed hydrodynamic model

The tidal array parameterisation in §3(b) was applied to the model in 17 different locations to simulate different energy extraction scenarios. The hydrodynamics-only model was set up to run for one spring-neap cycle (14.8 days). The spring-neap cycle chosen was from 14 August 2009 to 28 August 2009 with the spring tide occurring in the middle of the model run. This period was chosen because the model was primarily validated using ADCP data collected during 2009 and the cycle is one of the largest cycles of the year. The model is therefore conservative in that it represents the impacts of energy extraction during a period of higher-than-average tidal

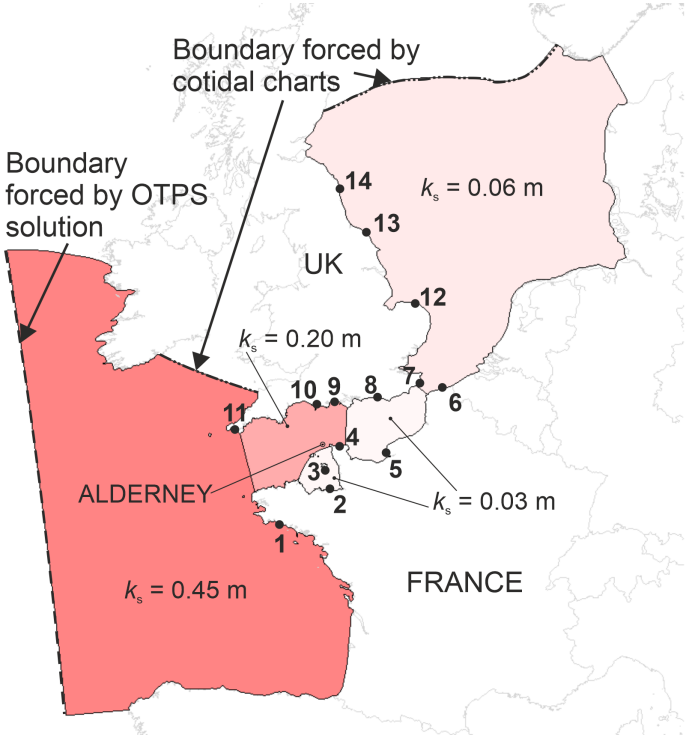

Figure 3: Overview of mesh and boundary counditions used in hydrodynamic model. See Table 3 for details of errors at the different numbered tide gauge locations

velocities. Residual sediment transport rates across the South Banks were calculated using the Soulsby-Van Rijn equations (Equation 3.1).

$$\begin{aligned} q_t &= q_b + q_s, \\ q_b &= 0.005\,\overline{U}h\left\{\frac{\overline{U}-\overline{U}_{cr}}{[(s-1)g\,d_{50}]^{0.5}}\right\}^{2.4}\left(\frac{d_{50}}{h}\right)^{1.2}, \\ q_s &= 0.012\,\overline{U}h\left\{\frac{\overline{U}-\overline{U}_{cr}}{[(s-1)g\,d_{50}]^{0.5}}\right\}^{2.4}\left(\frac{d_{50}}{h}\right)(D_*)^{-0.6} \end{aligned} \tag{3.1}$$

Where q_t is the total-load, q_b is the bedload, q_s the suspended-load, $\overline{U}$ the depth-averaged flow velocity, $\overline{U}_{cr}$ is the critical depth-averaged flow velocity, h water depth, d_{50} median grain size, g acceleration due to gravity, s the ratio of sediment density to water density, D_*, dimensionless grain size. The depth-averaged critical velocity, U_cr, determines the sediment threshold of motion and is defined using one of two different formulations relating to sediment size (Equation 3.2).

$$\begin{aligned} \overline{U}_{cr} &= 0.19\ (d_{50})^{0.1}\log_{10}\left(\frac{4h}{d_{90}}\right), 0.1 \leq d_{50} < 0.5\text{mm} \\ \overline{U}_{cr} &= 8.5\ (d_{50})^{0.6}\log_{10}\left(\frac{4h}{d_{90}}\right), 0.5 \leq d_{50} \leq 2\text{mm} \end{aligned} \tag{3.2}$$

Where d_{90} is the grain size for which 90% of the grains are finer. The residual sediment transport rates calculated from the numerical model were compared with those calculated from observed

sandwave migration over a 50-day period using Equation 3.3.

$$q_b = a_m H V_m, \qquad a_m = \zeta(1-\epsilon) \tag{3.3}$$

where q_b is the bedload, H is the bed feature height and V_m the rate of migration of the bedforms. The bedform factor a_m relates to the settled sediment porosity ϵ and a shape factor ζ for the bedform.

Sediment grain-size parameters of $d_{50} = 1.11$ mm and $d_{90} = 2.3$ mm were derived from the sediment survey grab samples and defined in SISYPHE for the sediment modelling phase, fixed for the whole domain. These values are the mean of the eight most North-Easterly samples collected at the South Banks (located within the dotted line in Figure 2). The sorting process that results in a significant increase in grain-size towards the South-Westerly end of the Banks (d_{50} values of 1.59 and 2.39 mm) was not able to be represented by the sediment model and therefore transport rates in this region will be overestimates (see Equations 3.1 and 3.2). The three sediment grabs in this region were not incorporated in the averages as it was considered more important to maintain a realistic average for the larger area of the Banks across which grain sizes fluctuate less, than to skew grain sizes for the whole sandbank.

(d) Coupled sediment transport model

A set of coupled hydrodynamic-sediment transport model-runs were also performed for a longer 90-day period using SISYPHE coupled two-way with TELEMAC-2D. The mesh was updated every five time steps by SISPYPHE and the results passed back to the hydrodynamic module. A non-erodible bed was used to limit potential erosion depths within the sediment model and to ensure realistic sediment supply, similarly to [8] and in contrast to [5]. This also prevents localized scour from taking place in the model around arrays, which would be unrealistic due to the area-averaged drag approximation for the turbines and in any case would occur in rocky areas without significant sediment present. The default active layer thickness for SISYPHE was used, $3d_{50}$.

The South Banks are situated on top of two separate bedrock strata with a marked step transition of 8 m between them. Separate spline interpolations beneath the sandbank were made for these two regions and combined to produce a continuous bedrock layer. This was then combined with the bathymetry for the wider domain and applied as a model-wide rigid bed layer (see perspective view in Figure 5). Only model nodes situated within this dotted red line were able to erode and the sediment supply to the morphological model is therefore limited to sand originating from the sandbank. In practical terms, two meshes were supplied to the model, one rigid and the other erodible; where the latter had a greater elevation, the mesh was allowed to 'erode'.

The sediment model was set up to run for a longer time-period than the hydrodynamics-only model to help investigate cumulative impacts on a larger time scale. A model run of 90 days (3 months) was chosen and was situated symmetrically in time around the hydrodynamic-only modelling period (i.e. July-September 2009). The model run encompasses six spring-neap cycles with the main outputs consisting of bed evolution time-series for each node of the model mesh.

4. Results and Discussion

(a) Validation of baseline numerical model

The modelled tidal elevations were analyzed harmonically using T_TIDE [26] and constituents compared with those derived from tide gauge records at eleven ports in the English Channel (Concarneau, Saint Malo, Jersey, Cherbourg, Le Havre, Dunkirk, Dover, Newhaven, Bournemouth, Weymouth and Newlyn) and a further three ports in the North Sea (Cromer, Whitby and North Shields). UK port tide gauge data were obtained from NTSLF and French

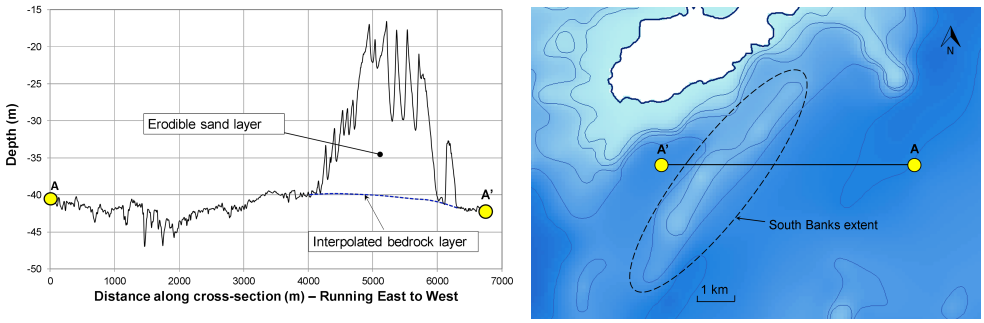

(a) Cross-section A-A' (b) Location of cross-section A-A'

Figure 4: A cross-sectional profile of the South Banks, illustrating how the unerodible bed was interpolated beneath the Banks

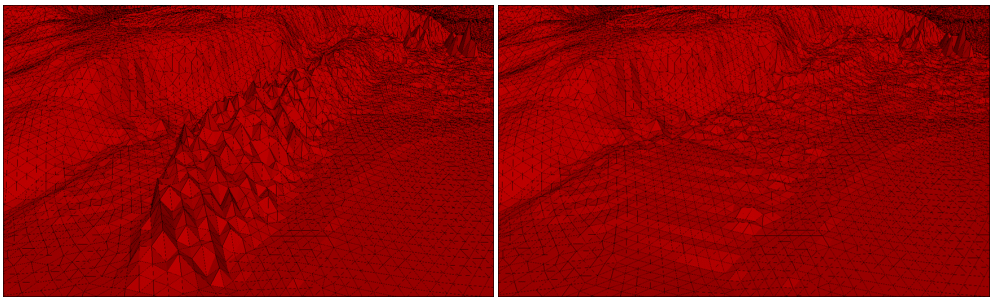

(a) Mesh including erodible volume (b) Mesh with erodible volume removed

Figure 5: A perspective view of the model mesh of the South Banks, viewed from the South West with vertical exaggeration, illustrating how the unerodible bed was interpolated beneath the Banks.

ports from SONEL. Table 3 shows the comparison for the two main constituents, M_2 and S_2. It can be seen that amplitude agreement is very good and phase error is within 10 degrees with the exception of Bournemouth where M_2 and S_2 amplitudes are small and non-linear tides dominate. Current profiles from five ADCP deployments carried out for Alderney Commission for Renewable Energy were analyzed and compared with the depth-averaged currents from the model; the differences are tabulated in Table 4. The agreement for M_2 tidal ellipse parameters (major axis, phase and inclination) was very good, less so for S_2. However the M_2 constituent typically accounts for 80% of tidal dissipation in this part of the continental shelf [27] and therefore overall the currents were reproduced well by the model.

(b) Energy extraction areas

The results of the baseline model were used to select a subset of 17 Alderney tidal development blocks (1 nm×1 nm blocks designated T1–96 and indicated in Figure 7a) of interest for tidal current power generation, using the cube-root-mean-cube of the depth-average flow speed $\left(\sqrt[3]{<\overline{U}^3>}\right)$ as a threshold. While this is not a reliable metric for the available resource [28,29], it nevertheless highlights areas where a single large array would generate high power. The selected

Table 3: Errors in tidal elevation constituents at tide gauges in the model domain (modelled versus actual). Number refers to location on Figure 3

		M_2			S_2		
		Amp.		Phase	Amp.		Phase
	Location	(m)	(%)	(deg)	(m)	(%)	(deg)
1	Concarneau	0.03	1.7	-6.3	0.04	7.3	-7
2	Saint-Malo	0.33	8.9	4	0.07	4.8	6.4
3	Jersey	0.19	5.7	4.3	0.01	0.4	5.5
4	Cherbourg	-0.13	-7	-1.8	-0.05	-7.3	-1.9
5	Le Havre	-0.18	-6.9	5.5	-0.08	-8.6	5
6	Dunkirk	-0.29	-13.4	-0.1	-0.11	-16.3	1.1
7	Dover	-0.06	-2.8	4.9	-0.04	-5.8	6.4
8	Newhaven	-0.12	-5.3	6.3	-0.06	-8.6	5.9
9	Bournemouth	-0.13	-32.4	-23.1	-0.01	-5.3	-18.6
10	Weymouth	0.15	25	-8.1	0.04	14.6	-5
11	Newlyn	-0.1	-6.1	0.4	-0.02	-4.3	-1
12	Cromer	-0.01	-0.8	-4.2	-0.05	-9.4	-5
13	Whitby	0.03	2	-8.7	0.01	1.6	-11
14	North Shields	-0.01	-0.9	-6.9	0	0.7	-9.1

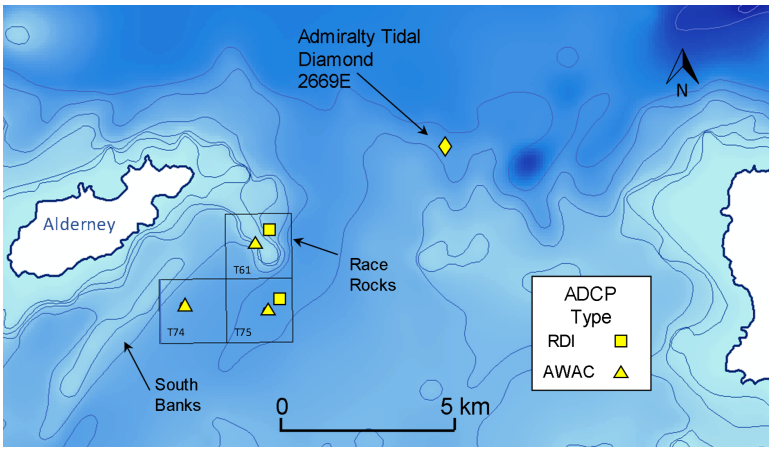

Figure 6: Locations of ADCP and Admiralty Tidal Diamonds used for validation of baseline hydrodynamic model. See Table 4 for details of errors at the different locations

areas are indicated in Figure 7b as rectangles aligned to the major axis of the M_2 ellipse. Note the high velocity area on the right of the image lies outside of Alderney territorial waters.

(c) Static bed model

Figure 8a illustrates the baseline residual sediment transport vectors as calculated from the model using Equations 3.1-3.2; the clockwise rotation of the vectors around the South Banks can be clearly seen. Figure 8b zooms in on four areas where repeated survey occurred. Table 5 gives a comparison between the sediment transport rates as estimated from observed sandwave migration and that calculated from the model. Note that sandwave migration tends to underestimate bedload sediment transport (q_b), as sand grains may roll over more than one sandwave, or be carried into suspension. In [18] it is suggested that the underestimate may be

Table 4: Errors in depth-averaged tidal current ellipse parameters. Note 'RDI' refers to an RDI Workhorse, 'AWAC' to and 'ATD' an Admiralty Tidal Diamond. For locations, please see Figure 6.

		M_2			S_2				
		Maj. axis		Phas.	Incl.	Maj. axis		Phas.	Incl.
Location	Type	**(m/s)**		**(%)**	**(deg)**	**(deg)**	**(m/s)**	**(%)**	**(deg)**	**(deg)**
T61a	RDI	0.08		2.9	3.9	-0.9	0.58	138.1	0.5	2
T61b	AWAC	-0.06		-2.3	0.2	-7.36	0.47	97.9	-3.2	-9.5
T75a	RDI	0.06		2.7	2.9	-0.3	0.4	94.6	5.3	-1.4
T75b	AWAC	0.14		6.4	2.9	13.05	0.41	100	0.3	13.1
T74b	AWAC	-0.11		-6.7	-0.1	3.7	-0.13	21.2	29	2.6
2669E	ATD	0.11		5.9	9.9	-5	-0.09	-13.4	3.7	-6.2

up to a factor of around two. Additionally, total load (q_t; bedload plus suspended load) can be estimated from the bedload given the water depth and sediment properties. Sediment transport rates for our model match those inferred from the sandwave migrations very well for analysis region 4 with almost identical residual direction and very similar total load values observed. Differences in region 3 are also fairly small. In analysis region 2 the directionality of the residual is wrong by around 30° and the magnitudes an under prediction by $\approx 30\%$. Discrepancies are at a maximum in region 1 where the directionality is almost 100° out and the magnitudes an underestimate by $\approx 40\%$. The increasing disparity towards the North-East of the bank appears to be due to the effects of the residual eddy and its specific location relative to the bank crest (see below). There are a number of potential inaccuracies introduced with such a comparison for example likely difference of directionality between q_b and q_s residuals, varying proportions of q_s and q_b) but the method represents the only means available for checking the realism of the model transport rates. It is interesting to note that in [5], $\ln()$ was used in error instead of $\log_{10}()$ in Equation 3.2 which led to an overestimate of critical velocity $\overline{U}$ and underestimated sediment transport rates by a factor of between two and six.

Table 5: Estimated bed and total load magnitude and direction for analysis regions 1–4 in Figure 8b

	Sandwave migration analysis (observed)			**Sediment transport residual (model)**	
	q_b	Approx. q_t	Dir.	q_t	Dir.
	m^2/day	$(5.6q_b)$	(deg)	m^2/day	(deg)
1	0.99	5.49	251.6	3.22	344
2	0.77	4.28	256.4	2.97	284.8
3	0.64	3.55	257.6	4	250.8
4	0.78	4.32	241.3	4.15	241.5

(d) Flow velocity changes under energy extraction scenarios

Flow speed differences for all seventeen cases are plotted in Figure 9 for the time step when the ambient ebb flow was strongest (spring ebb tide).

The downstream profile of the velocity deficit behind the arrays is consistently related to their lateral position relative to the South Banks. The deficit downstream from T47 is transported along a curved path passing over the middle of the South Banks. Deficits downstream from T48 follow a less curved path and those downstream from T49 curve a little in the opposite direction. The same pattern can be observed along rows T60–T63, T74–T76 and T85–87. This makes intuitive

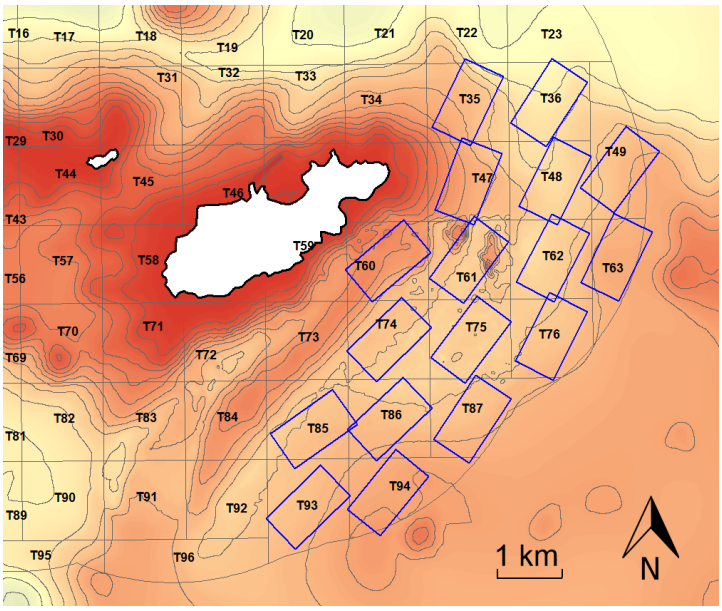

(a) Modelled array footprints displayed as blue inclined rectangles while Tidal development 'T-blocks' (licensing areas) are represented by the fainter grid. With indicative bathymetric contours

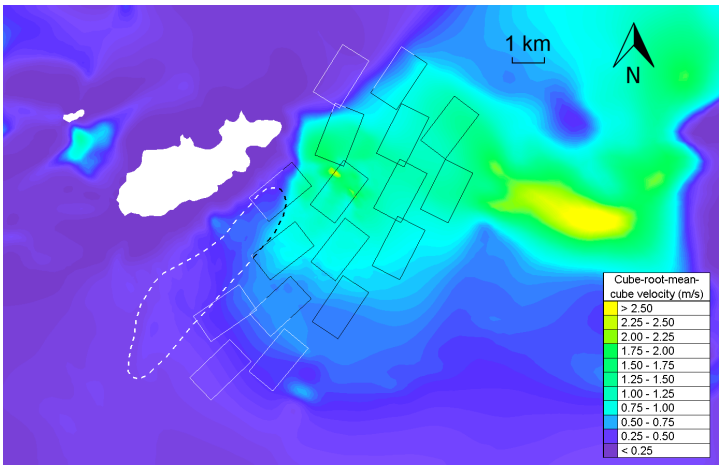

(b) Cube-root-mean-cube speeds for the baseline model

Figure 7: Selection of tidal turbine array areas. Array footprints included as blue rectangles and the South Banks limits marked by the dashed line.

sense if the large ebb-flows in this region are understood as acceleration around a blockage in the flow in i.e. the island of Alderney.

Lateral array location appears to significantly affect the magnitude of the downstream velocities in some cases. The T86 and T94 deficits are larger than the T85 and T93 values respectively. This is related to two factors. Velocities decrease with distance from the Race Rocks region so arrays situated further West are in fact located further downstream (i.e. T85 is further downstream than T86). Potentially more significant, ebb-tide velocity values increase with

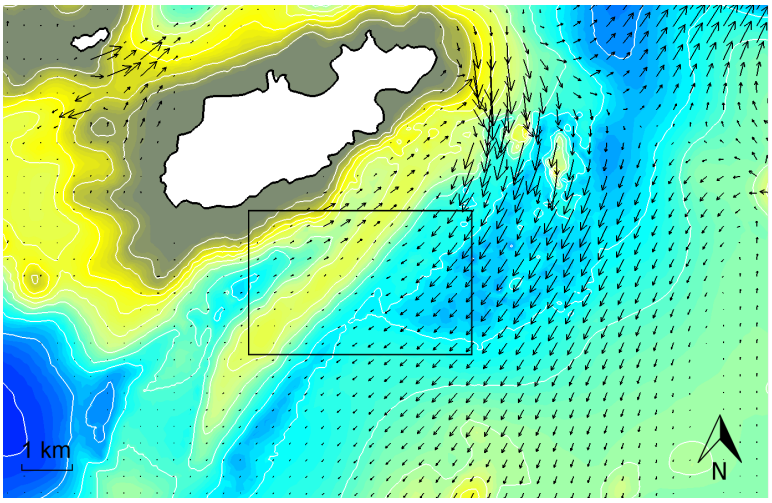

(a) Residual sediment transport rates around Alderney South Banks

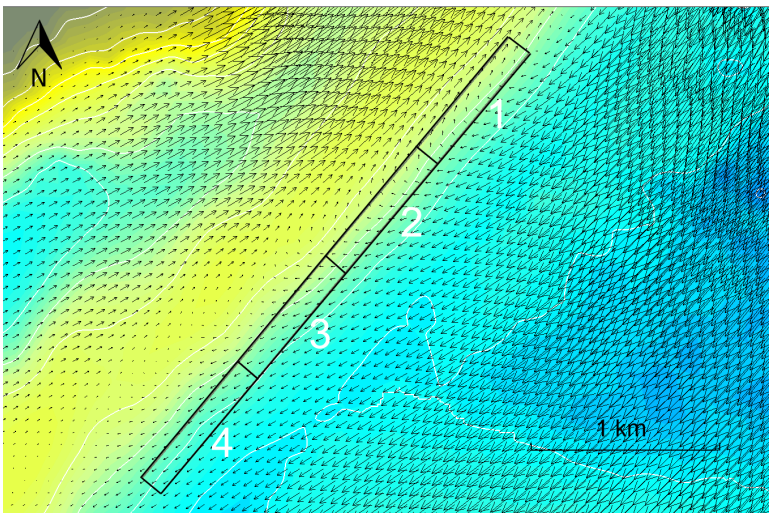

(b) Zoomed-in view of analysis regions 1–4 where repeated bathymetric survey indicated sandwave migration rates.

Figure 8: Residual sediment transport for the static bed baseline model. Velocity vectors were combined with the Soulsby-Van Rijn total-load transport formula [18] to produce instantaneous sediment transport rate vectors for each time-step. Rates were then vector-averaged across the 14.8 day run-period to produce the residual. Values mapped onto a rectilinear mesh (i.e. arrow locations do not imply mesh resolution).

distance from the sandbank. T86 and T94 are therefore situated in a stream of higher ebb-tide velocities (than T85 and T93 respectively) resulting in larger downstream velocity deficits.

Energy extraction in T74 can be seen to produce velocity deficits of > 0.2 m/s up to 9 km downstream from the array. Increased flow speed of up to 0.3 m/s can also be observed to the North-West of the array (over the South Banks), with maximum increase of ≈ 0.5 m/s occurring close to the centre of the propagating eddy. Flow acceleration around arrays is typically of much smaller magnitude to the deceleration produced immediately downstream of an array. Flow increases to the North-West of the T74 array are particularly high (compared to typical flow

increases of ≈ 0.1 m/s around arrays in an unbounded flow). This is due to the way in which flows reinforce the clockwise circulation of the eddy to the South of the eddy centre. Above this region there is another region of flow deceleration where acceleration around the array counteracts the clockwise motion of the eddy.

The T35 and T36 arrays affect flow speeds less than many of the other arrays. This is because flow velocities are smaller in this region resulting in flow speed decreases and increases of $<$ 0.2 m/s.

(e) Residual sediment transport under energy extraction scenarios

Figure 10 illustrates the difference in residual sediment transport under two energy extraction scenarios, T74 and T86. These array locations are geographically close (< 1 km), but the effects on residual sediment transport are very different. The difference in residual sediment transport between the baseline and T86 extraction scenario is plotted in Figure 10a. The South Banks have been split into zones of ebb and flood dominance to aid interpretation of the vector-differences. The difference vectors point to the South-West along the ebb-dominant South-Eastern flank of the sandbank suggesting that residual transport rates will increase relative to the baseline (see Figure 1 and Figure 8). Along the North-Western flood-dominant flank of the sandbank the vector-differences also point South-West away from the headland. This implies that the residual rates will decrease (as sediment transport is in the opposite direction). The magnitudes of difference on both sides of the bank are larger towards the North-East end of bank where the flow is more energetic and sediment transport rates are higher.

For the T74 extraction scenario (Figure 10b) the residual transport differences are significantly larger with a maximum difference of 10 m^2/day (occurring near to the sandbank crest adjacent to the array). This corresponds, at this location, to a residual transport rate reduction from 24 m^2/day to 16 m^2/day and to an anti-clockwise rotation from 54° to 45°. For this scenario extraction reduces transport rates on both sides of the sandbank (i.e. differences are in opposite direction to real-world sand movement) although the pattern is not symmetrical. Such modifications to the residual sediment transport would be likely to have significant impact upon the South Banks morphology and related equilibrium behaviours.

(f) Coupled sediment transport model

A steady state was not reached during the 90-day baseline simulation period, so the coupled sediment transport model results could only give qualitative indications of short term changes that would occur under different energy extraction scenarios. Differences in bed level change relative to the baseline scenario, over the 90-day simulation period, are plotted in Figure 11 for two of the seventeen cases. It can be seen that the patterns of erosion rates are very sensitive to the proximity of the array to the banks. Energy extraction in T74 leads to much larger bed-level differences relative to the baseline case. In contrast to the T86 scenario the large deposition zone at the South-West of the sandbank sees less deposition than baseline case. The region immediately downstream of the T74 array on the ebb-tide sees a reduction in erosion rates (due to flow deceleration) and a subsequent relative increase in bed-levels.

(g) Impact rankings

The 17 extraction scenarios were ranked using a composite index determined by the sum of three types of impact quantified as differences between baseline and extraction model runs, averaged over the footprint of the South Banks, scaled to the maximum spatial average value for that variable. The three variables are listed below in order of increasing complexity:

(i) Residual current: Variations in flow field over the sandbank were quantified and represent the most fundamental value for assessing impacts. It is the simplest measure to visualize, but least directly linked to sediment transport.
(ii) Residual sediment transport: The hydrodynamic outputs were converted to instantaneous sediment transport rates using sediment transport formulae. Averaged to produce residuals, these values interpret the model output velocities in terms of resultant sediment movement.
(iii) Bed level evolution: Evolution of the seabed, simulated using a sediment transport model, convert variations in sediment transport rates to modifications in sand movement and, subsequently, changes to the bathymetry.

The South Banks were divided into zones A–G plus the hypothesized sediment pathway (labelled SP) on Figure 12. For each zone and energy extraction scenario, the variables above were averaged and are indicated by a colour scale in Table 6. The lowest impacts are indicated by a purple colour ranging to yellow for the highest. It is immediately clear from Table 6 that the extraction scenarios with the most impacts are T47,T60,T74 and the scenarios with the lowest are T36 and T63. The pattern is generally consistent across the three variables, i.e. a high average impact in one variable is reflected in high average impacts in the other variables. However, comparing the results for sediment transport residual with bed evolution difference highlights some differences in which zone is most affected under a particular energy extraction scenario. Given the uncertainties involved, it is safest to draw conclusions at the level of the South Banks as a whole, but be mindful of the need for long term coupled sediment transport modelling to establish patterns of effects across the Banks. For the South Banks as a whole, the impact index for all scenarios is plotted in Figure 7 and the locations are also plotted on Figure 12; the scenarios were further assigned an impact category from I–III (with I indicating highest impact and III lowest). The categories are indicated on Figure 13 and further described in Table 7.

Arrays located close to the North-Eastern tip of the South Banks result in the highest impacts to the flow regime and, consequently, the largest impacts upon sandbank morphology. Development and lifetime of the large propagating eddy shed from the island is particularly sensitive to array installation in this area (Figure 1). Impacts decrease with distance from this region with arrays located the furthest East leading to the minimum variations over the banks (T63, T49 and T36). Arrays situated in these locations have a comparatively small effect on the banks during the ebb-tide due to their distance from the headland where the flow divides around Alderney. Crucially, these same arrays are also situated too far downstream from the sandbank (i.e. not adjacent to the South Banks) on the flood-tide and therefore have an almost negligible effect during this phase of the tide.

5. Conclusion

Many of the high energy locations within Alderney waters would be unlikely to significantly affect the flow velocities around the South Banks, if a single large array were installed at that location (work is ongoing to investigate multi-array interactions). However for certain locations, the simulations suggest that the potential for asymmetrical modifications to the flow regime, and hence to the sedimentary regime, is high. Areas of flow decrease downstream of tidal device arrays will only occur on one phase of the tidal cycle (either flood or ebb). The hydrodynamic results indicate that the South Banks will experience relative flow deceleration from the modelled arrays on the ebb-tide predominantly. Flow acceleration around arrays may also have an important impact at specific array locations. Although acceleration effects around arrays are typically smaller than deceleration effects downstream of arrays, they may be induced in the region of the South Banks on both the ebb and flood tides thereby increasing the impact of such acceleration effects. A limitation of this work has been the exclusion of wave effects which may lead to variability in sediment transport of similar magnitude to that than from energy extraction [8]. This work has also been limited to potential arrays of turbines installed in

Alderney waters; however if eventually large arrays are installed throughout Alderney Race/Raz Blanchard, significant flow changes are likely to occur throughout the region [30]. This will require cross-border co-operation to assess—and if necessary mitigate—risks to the maintenance of the Alderney South Banks.

Data Accessibility. The model configuration files, including steering, boundary conditions and fortran files (but not bathymetry, due to licence restrictions), for all the simulations described in this paper are available at https://doi.org/10.5258/SOTON/D1240

Authors' Contributions. LB designed the study, drafted and edited the manuscript. SH performed the data analysis, generated the figures and drafted the manuscript. AB conceived of and oversaw the study, and edited the manuscript. All authors read and approved the manuscript.

Competing Interests. The authors declare that they have no competing interests.

Funding. This work is part of the activities of the Energy and Climate Change Division and the Sustainable Energy Research Group in the Faculty of Engineering and Physical Sciences at the University of Southampton www.energy.soton.ac.uk, UK. Part of the funding for this work was provided by the Alderney Commission for Renewable Energy. It was also supported by EPSRC grants EP/K013319/1 (Reducing the Costs of Marine Renewables), EP/K012347/1 (International Centre for Infrastructure Futures) and EP/R030391/1 (Clustering Mini-Grid Networks). The work also received support from a British Council Institutional Links grant (University of Southampton - University of San Carlos, 2017)

Acknowledgements. Part of the bathymetric and tidal current datasets used in this work were provided by Alderney Commission for Renewable Energy.

Disclaimer. The views expressed are those of the authors and do no imply endorsement by other organizations. The images should not be used for navigational purposes.

References

1. Fairley I, Masters I, Karunarathna H. 2015 The cumulative impact of tidal stream turbine arrays on sediment transport in the Pentland Firth.
Renewable Energy **80**, 755–769.
2. Martin-Short R, Hill J, Kramer SC, Avdis A, Allison PA, Piggott MD. 2015 Tidal resource extraction in the Pentland Firth, UK: Potential impacts on flow regime and sediment transport in the Inner Sound of Stroma.
Renewable Energy **76**, 596–607.
3. Chatzirodou A, Karunarathna H, Reeve DE. 2017 Modelling 3D hydrodynamics governing island-associated sandbanks in a proposed tidal stream energy site.
Applied Ocean Research **66**, 79–94.
4. Bastos A, Collins M, Collins N. 2003 Water and sediment movement around a coastal headland: Portland Bill, southern UK.
Ocean Dynamics **53**, 309–321.
5. Neill SP, Jordan JR, Couch SJ. 2012 Impact of tidal energy converter arrays on the dynamics of headland sand banks.
Renewable Energy **37**, 387–397.
6. Neill S, Robins P, Fairley I. 2017 The Impact of Marine Renewable Energy Extraction on Sediment Dynamics.
In *Marine Renewable Energy* (ed. Z Yang, A Copping), pp. 279–304. Cham, Switzerland: Springer.
7. Neill SP, Litt EJ, Couch SJ, Davies AG. 2009 The impact of tidal stream turbines on large-scale sediment dynamics.
Renewable Energy **34**, 2803–2812.
8. Robins PE, Neill SP, Lewis MJ. 2014 Impact of tidal-stream arrays in relation to the natural variability of sedimentary processes.
Renewable Energy **72**, 311–321.
9. Evans EM. 1987 *Tidal stream energy*.
Ph.D. thesis, Plymouth Polytechnic.

10. Bahaj AS, Myers L. 2004 Analytical estimates of the energy yield potential from the Alderney Race (Channel Islands) using marine current energy converters.
Renewable Energy **29**, 1931–1945.
11. Blunden L, Bahaj A. 2007 Tidal energy resource assessment for tidal stream generators.
Proceedings of the Institution of Mechanical Engineers, Part A: Journal of Power and Energy **221**, 137–146.
12. Coles DS, Blunden LS, Bahaj AS. 2017 Assessment of the energy extraction potential at tidal sites around the Channel Islands.
Energy **124**, 171–186.
13. Thiébot J, Bailly du Bois P, Guillou S. 2015 Numerical modeling of the effect of tidal stream turbines on the hydrodynamics and the sediment transport - Application to the Alderney Race (Raz Blanchard), France.
Renewable Energy **75**.
14. Dyer KR, Huntley DA. 1999 The origin, classification and modelling of sand banks and ridges.
Continental Shelf Research **19**, 1285–1330.
15. Bastos AC. 2002 *Sedimentary processes and deposits associated with a coastal headland: Portland Bill, Southern UK.*
Ph.D. thesis, University of Southampton School of Ocean and Earth Sciences.
16. Bastos AC, Paphitis D, Collins MB. 2004 Short-term dynamics and maintenance processes of headland-associated sandbanks: Shambles Bank, English Channel, UK.
Estuarine, Coastal and Shelf Science **59**, 33–47.
17. Neill SP. 2008 The role of Coriolis in sandbank formation due to a headland/island system.
Estuarine, Coastal and Shelf Science **79**, 419–428.
18. Soulsby RL. 1997 *Dynamics of marine sands*.
HR Wallingford; Thomas Telford Publications.
19. Morelissen R, Hulscher SJMH, Knaapen MAF, Németh AA, Bijker R. 2003 Mathematical modelling of sand wave migration and the interaction with pipelines.
Coastal Engineering **48**, 197–209.
20. Knaapen MAF. 2005 Sandwave migration predictor based on shape information.
Journal of Geophysical Research: Earth Surface **110**.
21. Hervouet JM. 2007 *Hydrodynamics of Free Surface Flows*.
John Wiley and Sons, Ltd.
22. Egbert GD, Erofeeva SY, Ray RD. 2010 Assimilation of altimetry data for nonlinear shallow-water tides: Quarter-diurnal tides of the Northwest European Shelf.
Continental Shelf Research **30**, 668–679.
23. Howarth MJ. 1990 Atlas of tidal elevations and currents around the British Isles.
Technical Report OTH–89-293, Department of Energy.
24. IOC, IHO, BODC. 2003.
Centenary Edition of the GEBCO Digital Atlas.
Published on CD-ROM.
25. Blunden L. 2009 *New approaches to tidal stream energy analysis at sites in the English Channel*.
Ph.D. thesis, University of Southampton.
26. Pawlowicz R, Beardsley R, Lentz S. 2002 Classical tidal harmonic analysis including error estimates in MATLAB using T_TIDE.
Computers and Geosciences **28**, 929–937.
27. Pugh DT. 1987 *Tides, surges and mean sea-level. A handbook for Engineers and Scientists*.
John Wiley & Sons.
28. Garrett C, Cummins P. 2005 The power potential of tidal currents in channels.
Proc. R. Soc. Lond. A **461**, 2563–2572.
29. Vennell R, Funke SW, Draper S, Stevens C, Divett T. 2015 Designing large arrays of tidal turbines : A synthesis and review.
Renewable and Sustainable Energy Reviews **41**, 454–472.
30. Coles DS, Blunden LS, Bahaj AS. 2020 Updated estimate of the energy yield potential of a large tidal stream turbine array in Alderney Race (Channel Islands).
Philosophical Transactions of the Royal Society A: Mathematical, Physical and Engineering Sciences.
Submitted to journal.

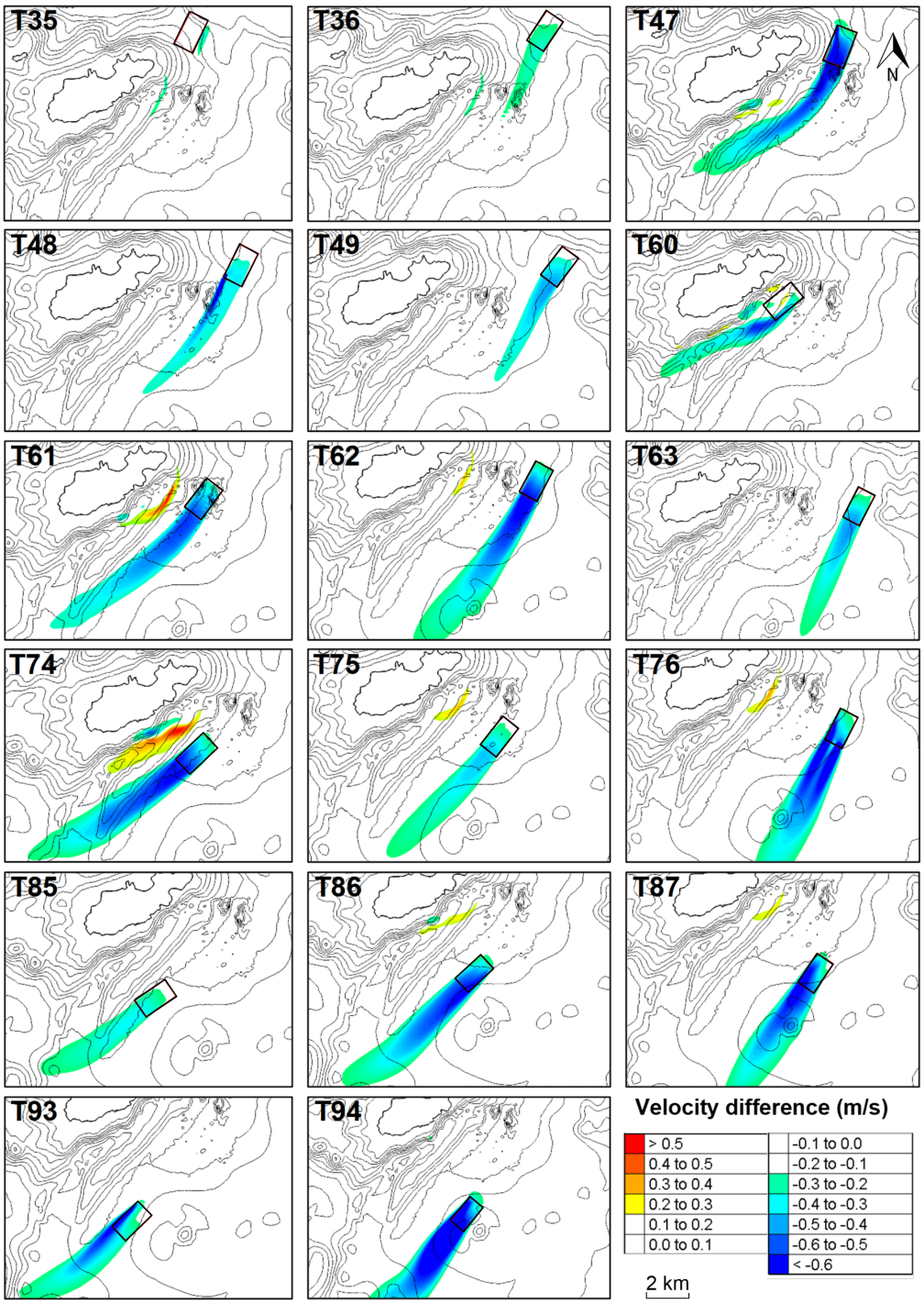

Figure 9: Flow speed differences for seventeen 300 MW energy extraction scenarios (indicated in Figure 7a). Identical colour scales are used to aid inter-scenario comparison. Outputs are all for the same equivalent model-time step and relate to the ebb-spring-tide (the largest tidal-cycle of the model run). Array footprints are highlighted in purple. Velocity differences $< \pm 0.2$ m/s are not shaded.

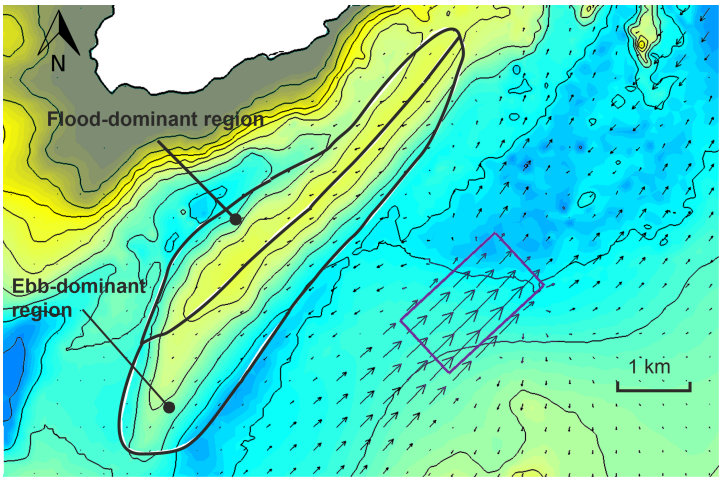

(a) T86 energy extraction scenario. Maximum magnitude of residual difference within the banks region is 4.1 m^2/day

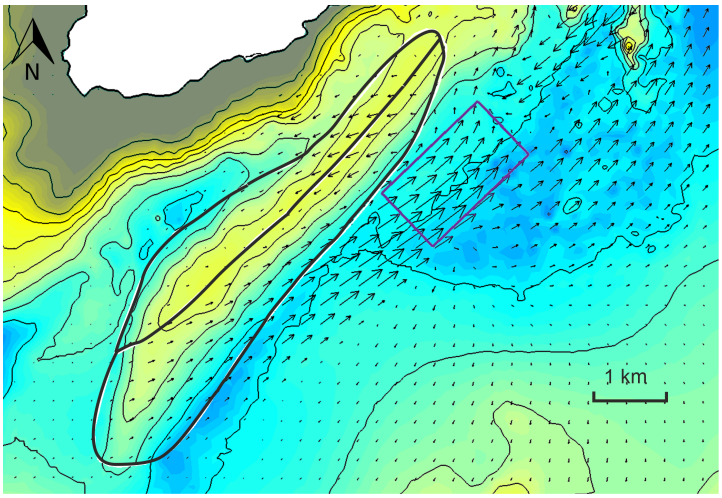

(b) T74 energy extraction scenario. Maximum magnitude of residual difference within the banks region is 10.0 m^2/day (Note this is different from T86).

Figure 10: Vector-difference in residual sediment transport between the baseline and energy extraction scenarios. The regions of ebb and flood dominance over the South Banks are outlined and divided (See Figure 1 for details). Array footprint highlighted in blue.

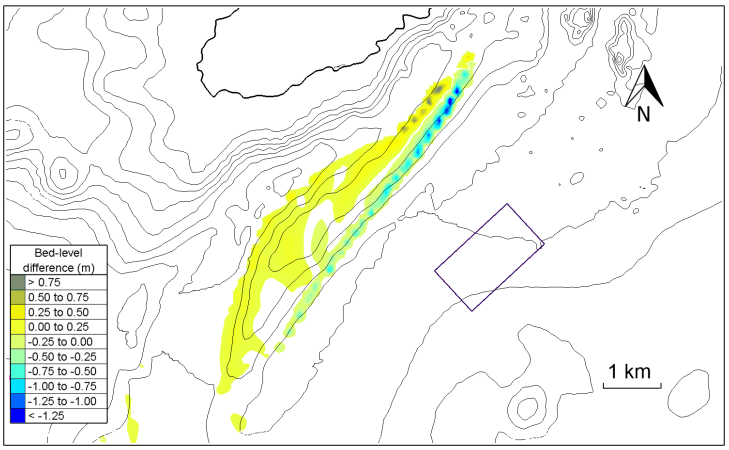

(a) T86 energy extraction scenario

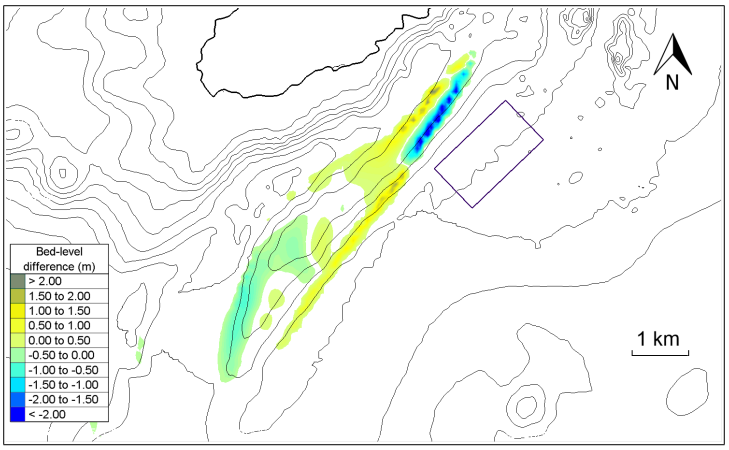

(b) T74 energy extraction scenario (note different colour scale)

Figure 11: Differences in bed elevation after 90-day model run under energy extraction scenarios. Location of simulated array indicated by blue rectangle. Note different colour scale for the two figures

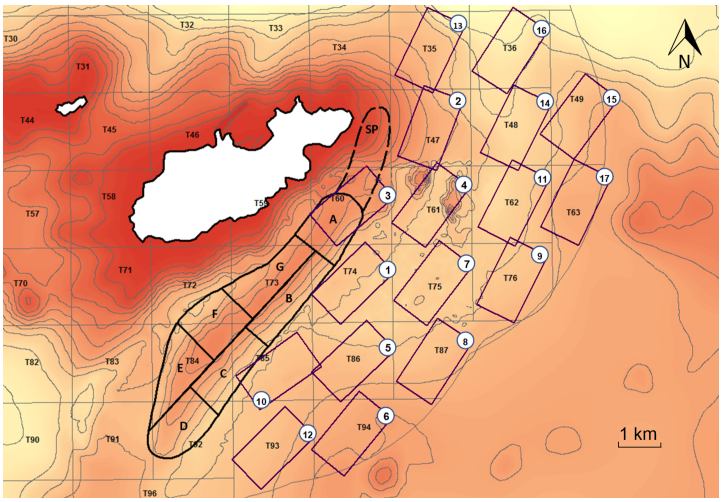

Figure 12: Array footprints for each development T-block (purple rectangles, black lettering) and the South Banks Zone limits (black lines, letters A–G plus sediment pathway 'SP'). The Impact Ranking (see Figure 13) for each 300 MW extraction scenario is included in the corner of the corresponding array footprint (Impact Ranking of 1 corresponds to largest impact).

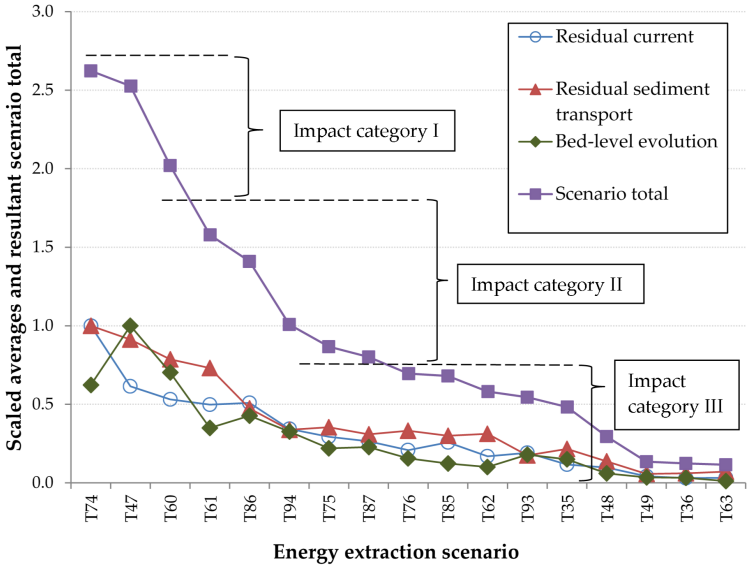

Figure 13: Scenario total for each of the 17 energy extraction scenarios. The scenarios are ordered from highest to lowest impact l-r. The scenario total is the sum of the three different types of average (residual current, residual sediment transport and bed-level evolution) that have each been scaled to the corresponding maximum value for all 17 scenarios (i.e. maximum = 1). The ranges corresponding to Impact Categories I, II and III are highlighted (see Table 7)

Table 6: Effects on different zones of the Alderney South Banks predicted from numerical modelling. The zones are defined in Figure 12. For each class of impact, purple colours indicate the least impact and yellow indicate the most impact. The ranges corresponding to Impact Categories I, II and III are highlighted (see Table 7)

		300 MW Array scenarios																	Keys			Statistics			
	Zones	T35	T36	T47	T48	T49	T60	T61	T62	T63	T74	T75	T76	T85	T86	T87	T93	T94	Value / unit	Zones key	Average key	Maximum	Minimum	Mean	Model run time
Velocity Residual Difference	A																								
	B																								
	C																		**Residual**	0.150					
	D																		**velocity**	0.125	0.10	0.15	0.00	0.03	15
	E																		vector	0.100	0.08				days
	F																		difference	0.075	0.06				
	G																		(m/s)	0.050	0.04				
	Sed. Path.																			0.025	0.02				
	Average																			0.000	0.00	**0.10**	**0.00**	**0.03**	
Sediment Transport Residual Difference	A																			8.0					
	B																		**Residual**	7.0	3.5				
	C																		**sediment**	6.0	3.0				
	D																		**transport**	5.0	2.5	8.85	0.04	1.43	15
	E																		**rate**	4.0	2.0				days
	F																		vector	3.0	1.5				
	G																		difference	2.0	1.0				
	Sed. Path.																		(m^2/day)	1.0	0.5				
	Average																			0.0	0.0	**3.70**	**0.21**	**1.43**	
Evolution Difference	A																								
	B																			0.6					
	C																		**Bed-level**	0.5					
	D																		**evolution**	0.4	0.175	0.58	-0.27	0.01	90
	E																		difference	0.3	0.150				days
	F																		(m)	0.2	0.125				
	G																			0.1	0.100				
	Sed. Path.																			0.0	0.075				
	Avg. Depos.																			-0.1	0.050	0.23	0.00	0.05	
	Avg. Erosion																			-0.2	0.025	-0.11	0.00	-0.04	
	Average																			-0.3	0.000	**0.17**	**0.00**	**0.05**	

Extraction scenarios	**T35**	**T36**	**T47**	**T48**	**T49**	**T60**	**T61**	**T62**	**T63**	**T74**	**T75**	**T76**	**T85**	**T86**	**T87**	**T93**	**T94**
Impact Ranking	**13**	**16**	**2**	**14**	**15**	**3**	**4**	**11**	**17**	**1**	**7**	**9**	**10**	**5**	**8**	**12**	**6**
Impact category	4	5	1	4	5	1	2	3	5	1	2	3	3	2	2	3	2

Table 7: Energy extraction scenarios grouped into three impact categories relating to the broad effects of array installation.

Impact Category	**Array located in T-Block:**	**Description**
I	T74, T60, T47	Significant impact on the eddy path and magnitude, large decreases or increases in flow speed occur directly over the South Banks
II	T61, T75, T86, T87, T94	Some impact on the eddy path and magnitude across South Banks
III	T85, T93, T62, T76, T35, T48, T49, T36, T63	Impacts occur in some zones, flow differences occur over the banks but are not large. Impact upon eddy is relatively small and upon the flow in general is localized.